


Article

Genomic Regions Associated with the Position and Number of Hair Whorls in Horses

Diogo Felipe Pereira de Assis Lima ¹, Valdecy Aparecida Rocha da Cruz ¹, Guilherme Luís Pereira ², Rogério Abdallah Curi ², Raphael Bernal Costa ¹ and Gregório Miguel Ferreira de Camargo ^{1,*} 

¹ Escola de Medicina Veterinária e Zootecnia, Universidade Federal da Bahia (UFBA), Salvador 40170-110, BA, Brazil; dflima@live.com (D.F.P.d.A.L.); valdecya.r.cruz@gmail.com (V.A.R.d.C.); raphaelbcosta@gmail.com (R.B.C.)

² Departamento de Melhoramento e Nutrição Animal, Universidade Estadual Paulista (Unesp), Botucatu 18618-681, SP, Brazil; guilherme.luis@unesp.br (G.L.P.); rogerio.curi@unesp.br (R.A.C.)

* Correspondence: gregorio.camargo@ufba.br

Simple Summary: Whorls have been used to indicate the temperaments of domestic animals; however, little is known about the biological events that drive this association. The present study is the first that aims to find the main genomic regions that influence the whorl traits in livestock, with horses as a model. Genes related to hair follicle growth were found. Interestingly, some of these genes also influence psychiatric diseases and neurological disorders, thus evidencing a consistent biological explanation for the association.

Abstract: The position and number of hair whorls have been associated with the behavior, temperament, and laterality of horses. The easy observation of whorls assists in the prediction of reactivity, and thus permits the development of better measures of handling, training, mounting, and riding horses. However, little is known about the genetics involved in the formation of hair whorls. Therefore, the aim of this study was to perform a genome-wide association analysis to identify chromosome regions and candidate genes associated with hair whorl traits. Data from 342 Quarter Horses genotyped for approximately 53,000 SNPs were used in an association study using a single-step procedure. The following traits were analyzed: vertical position of hair whorl on the head, number of whorls on the head, and number of whorls on the left and right sides of the neck. The traits had between one and three genomic windows associated. Each of them explained at least 4% of the additive variance. The windows accounted for 20–80% of additive variance for each trait analyzed. Many of the prospected genes are related to hair follicle growth. Some of these genes exert a pleiotropic effect on neurological and behavioral traits. This is the first indication of biological and physiological activity that might explain the association of hair whorls and temperament.

Keywords: behavior; hair follicle; Quarter Horse; SNP; temperament



Citation: Lima, D.F.P.d.A.; da Cruz, V.A.R.; Pereira, G.L.; Curi, R.A.; Costa, R.B.; de Camargo, G.M.F. Genomic Regions Associated with the Position and Number of Hair Whorls in Horses. *Animals* **2021**, *11*, 2925. <https://doi.org/10.3390/ani11102925>

Academic Editor: Heather Huson

Received: 10 September 2021

Accepted: 6 October 2021

Published: 10 October 2021

Publisher's Note: MDPI stays neutral with regard to jurisdictional claims in published maps and institutional affiliations.



Copyright: © 2021 by the authors. Licensee MDPI, Basel, Switzerland. This article is an open access article distributed under the terms and conditions of the Creative Commons Attribution (CC BY) license (<https://creativecommons.org/licenses/by/4.0/>).

1. Introduction

Quarter Horses have great visibility and economic importance, mainly due to their versatility in different equestrian modalities. The breed is subdivided into different populations according to their competencies, resulting from different selection objectives. The racing population has animals with the ability to run short distances, while the stock population is used in functional tests, exploring skills such as agility, temperament, obedience, and cow sense [1].

Horses are animals that are managed directly and routinely by humans. Behavioral differences are easily observed in this species [2]. However, the measurement of temperament traits is not always easy. A morphological mark that has been associated with temperament is the hair whorl. In horses, the vertical and lateral position, number, and direction of the growth of hair whorls on the head have been associated with behavior,

temperament, and laterality [3–6]. This association has been attributed to the fact that the epidermis and nervous system have the same embryonic origin [7].

Hair whorl traits in horses show high heritability [8–10] and are highly correlated with one another [10]. However, the genetic architecture of these traits and the biological mechanisms underlying their association with animal behavior are unknown. Therefore, the aim of this study is to perform the first genomic-wide association study (GWAS) of the vertical position of hair whorls on the head, in addition to the number of whorls on the head and neck in domestic animals, using horses as a study model. It will help to construct the first genetic–biological explanation of the association between whorls and temperament.

2. Materials and Methods

This study used 340 registered Quarter Horses of the racing line, 265 females and 75 males, born between 1985 and 2012. For the evaluation of whorl position, animals with hair whorls in more than one vertical position on the head were excluded, resulting in 252 females and 73 males.

The total sample was established to best represent the diversity of racing Quarter Horses in Brazil. Animals with many offspring, as well as descendants of individuals that were influential in the formation of the breed, were selected to be genotyped. Sampling of full siblings was avoided. The breeders of these animals agreed to the sampling and genotyping. The animal procedures were approved by the Ethics Committee on Animal Use of FMVZ, Unesp, Botucatu (protocol number 157/2014–CEUA).

The hair whorl phenotypes were obtained from the official identification document (outline diagram) kindly provided by the Brazilian Association of Quarter Horse Breeders (ABQM), which contains graphical and discretionary representations of the location of the marks that identify the animals (Figure 1).

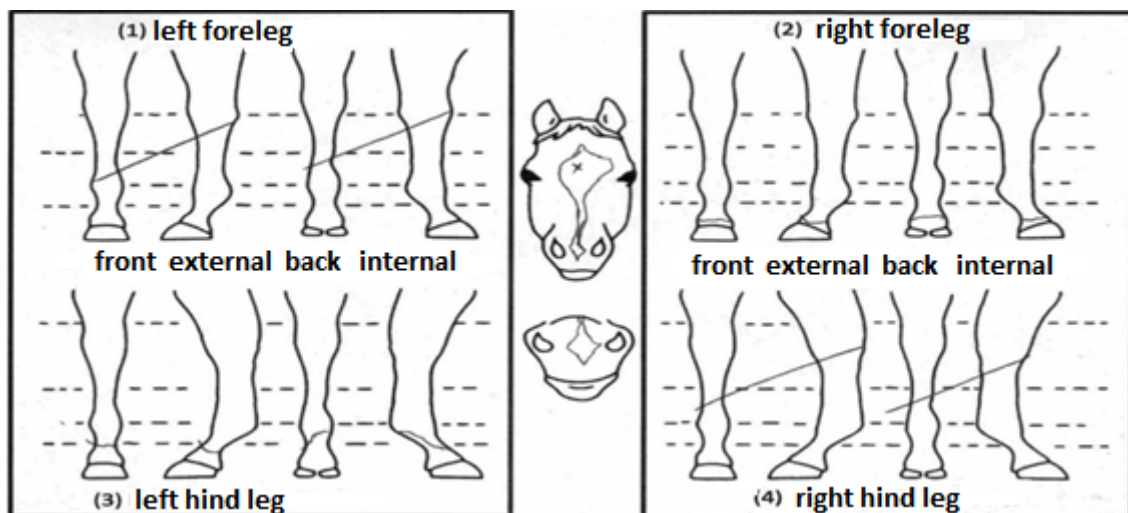


Figure 1. Official outline diagram from ABQM containing a graphic representation of the whorls' position and number (authors' own translation).

The following traits were studied: the position (POS) and number (NUM) of hair whorls on the head, and the number of hair whorls on the left (NUML) and right (NUMR) side of the neck. For POS, the horses were classified into three groups according to whorl position: (1) above the upper eye line; (2) between the upper and lower eye line; and (3) below the lower eye line. For NUM, the hair whorls arranged on the animal's head were counted, considering the head area to end at the appearance of the ears. For NUML and NUMR, the number of hair whorls located throughout the neck was counted, considering the appearance of the cranium and thorax as the upper and lower limits, respectively.

Preliminary analyses of data consistency and descriptive statistics were performed using the R package (<https://www.r-project.org>). Table 1 shows the descriptive statistics of the population. The systematic effects of sex and hair coat were tested in the model and were not significant ($p > 0.05$).

Table 1. Descriptive statistics of hair whorl traits in Quarter Horses.

Trait	Phenotype (No. of Animals)	Total No. of Animals
POS *	1(161), 2(144), 3(18)	323
NUM **	1(306), 2(32), 3(2)	340
NUML **	1(263), 2(65), 3(10), 5(2)	340
NUMR **	1(263), 2(65), 3(11), 7(1)	340

POS: position of hair whorls on the head; NUM: number of hair whorls on the head; NUML and NUMR: number of hair whorls on the left and right side of the neck, respectively. * For hair whorl position on the head, the phenotypes were divided as follows: (1) above the upper eye line; (2) between the upper and lower eye line; and (3) below the lower eye line. ** The number of hair whorls were counted on the outline diagram to obtain their numerical values.

Classes with few observations for NUM, NUMRL, and NUMR were also grouped to other classes to avoid low-incidence sampling problems. The analyses were re-run, and the results proved to be the same.

Genome-Wide Association Study

A number of the animals ($n = 120$) were genotyped with the Illumina Equine SNP50 BeadChip (54K) (Illumina Inc., San Diego, CA, USA) and the rest ($n = 240$) with the Illumina Equine SNP70 BeadChip (65K) (Illumina Inc., USA). Quality control of genotyped individuals and SNPs and genotype imputation were performed as described by [11]. Animals with a call rate of < 0.9 were excluded from the data set. SNPs located on the X-chromosome, SNPs with a call rate of < 0.9 , and SNPs with a p -value of $< 1 \times 10^{-5}$ for Hardy–Weinberg equilibrium were eliminated. The MAF was not initially used as an exclusion criterion of SNPs, since different ranges of MAF were applied to verify the efficiency of the two-step genotype imputation between the SNP50 and SNP70 equine chips. After quality control and imputation, 342 animals genotyped with 55,196 SNPs remained. The SNPs of the chip were annotated in the EquCab 2.0 genome assembly, and their position was updated to the most recent version of the genome assembly, EquCab 3.0. Some SNPs could not be aligned, and had to be excluded from the analysis, leaving 53,828 markers remaining.

Genomic association analysis was performed using four independent phenotypes: (1) POS; (2) NUM; (3) NUML; and (4) NUMR, in a single-trait model for each phenotype evaluated.

The threshold animal model without systematic effects assumes that the underlying (liability) scale has a normal continuous distribution as follows:

$$l_{ij} = a_i + e_{ij},$$

where l is the liability; a is the random effect of the animal; and e_{ij} is the residual random vector. The animal model using Bayesian inference assumes that $\sigma_a^2 \sim N(0, A \sigma_a^2)$ and $\sigma_e^2 \sim N(0, R \sigma_e^2)$, where σ_a^2 and σ_e^2 are the direct genetic and residual variance components, respectively; A is the numerator relationship matrix, and R is the variance matrix of the residual vector. The residual variance (σ_e^2) was set at 1. According to the Bayesian approach, liability is conditional on all parameters, and is thus independently distributed, allowing the estimation of mean breeding values different from zero. Convergence was evaluated by Geweke criteria that varied from 0.0 to 0.02 for the analyses.

Quality control of the SNPs after imputation was performed using PEGSF90 software [12] which considered a call rate of > 0.90 , a minor allele frequency of > 0.05 , and a Hardy–Weinberg equilibrium of < 0.15 . A total of 53,828 markers remained for GWAS.

Single-step GBLUP was used for analysis. The variance components were estimated with the THRGIBBS1F90 software [12], posterior means were obtained with POST-GIBBSF90 [12], and the POSTGSF90 software was used for the prediction of SNP effects, and for the generation of Manhattan plots.

The variations explained by windows comprising 100 adjacent SNPs were used to identify genome regions with a major effect on the traits evaluated. Major-effect genes present in the windows were prospected in the NCBI database (National Center for Biotechnology Information) using EquCab 3.0 as the reference genome, filtered by species, chromosome, and position of the window.

3. Results

The present results of GWAS of the position and number of hair whorls on the head and neck of horses are the first reported in the literature for domestic animals, using horses as a study model (Table 2). For the four traits studied, few genomic windows explained most of the additive genetic variation, as illustrated in the Manhattan plots shown in Figures 2–5.

Table 2. Genomic windows and percentage of additive genetic variance (V_a) in the four hair whorl phenotypes explained by each window.

Phenotype	Genomic Window (Chromosome: Start Position–End Position in bp)	V_a %
POS	17: 45,252,386–49,471,423	51.31
	2: 104,112,526–108,667,352	4.56
	5: 7,191,873–11,827,369	4.41
NUM	1: 54,370,083–58,251,385	26.80
	19: 49,710,771–53,302,322	6.46
	23: 17,020,869–20,697,071	4.25
NUML	5: 29,306,930–34,034,348	14.06
	11: 50,127,066–53,788,216	8.48
NUMR	7: 70,662,347–74,512,078	81.96

POS: position of hair whorls on the head; NUM: number of hair whorls on the head; NUML and NUMR: number of hair whorls on the left and right side of the neck, respectively.

For POS, three windows were found that explained more than 4% of the additive variance in the trait, in decreasing order: 51.31% (ECA17), 4.56% (ECA2), and 4.41% (ECA5) (Table 2). The sum of the variances explained by these windows was 60.28% of the total additive variance, resembling a qualitative trait, due to the large influence of few genomic regions on the trait.

Three windows that explained more than 4% of the additive genetic variance were also identified for NUM: 26.80% (ECA1), 6.46% (ECA19), and 4.25% (ECA23) (Table 2). The windows together explained 37.51% of the total genetic variance in the trait, following the pattern observed for POS.

The other two traits evaluated, NUML and NUMR, followed the same patterns of genetic architecture of the others: few genomic regions with a large influence on the trait. There were two windows explaining 14.06% (ECA5) and 8.48% (ECA11) of the additive genetic variance in NUML (sum of 22.54%), and only one window explaining 81.96% (ECA7) of the variance in NUMR (Table 2).

The genes were prospected according to their location in the genome, and arranged as shown in Table 3.

Table 3. Genes within significant windows for each trait.

Trait	Chromosome/Additive Variance Explained (%)	Gene (Symbol)
POS	ECA17 (51.31)	<i>KLF5, PIBF1, MZT1, KLF12, BORA, DACH1, LMO7, UCHL3, DIS3, TBC1D4, COMMD6</i>
	ECA2 (4.56)	<i>IL2, MIR147B, SMIM43, USP53, C2H4orf3, PDE5A, MAD2L1, PRDM5, NDNF, TNIP3, QRFPR, ANXA5, CCNA2, TRPC3, BBS12, NUDT6, EXOSC9, BBS7, KIAA1109, ADAD1, SPATA5, SPRY1, ANKRD50, FABP2, FGF2, IL21</i>
	ECA5 (4.41)	<i>FASLG, TNFSF4, MIR214, MIR199A, TNFSF18, TEX50, KIAA0040, RABGAP1L, COPI1, TNR, TNN, CACYBP, SERPINC1, DARS2, KLHL20, ANKRD45, SLC9C2, SUCO, C5H1orf05, PIGC, DNM3, MYOC, FMO1, FMO2, MROH9, PAPP2, MRPS14, RC3H1, CENPL, PRDX6, METTL13, VAMP4, PRRC2C, FMO4, FMO3, ZBTB37, GPR52</i>
NUM	ECA1 (26.80)	<i>SIRT1, VPS26A, HK1, SUPV3L1, DDX21, STOX1, TET1, SLC25A16, DNA2, MYPN, FAM241B, TSPAN15, SRGN, KIFBP, DDX50, CCAR1, HNRNPH3, RUFY2, PBLD, HERC4, DNAJC12, LRRTM3, CTNNA3, ATOH7, NEUROG3, HKDC1, TACR2</i>
	ECA19 (6.46)	<i>CD47, CD200, HHLA2, CCDC54, MYH15, TRAT1, BBX, IFT57, CIP2A, DZIP3, RETNLB, GUCA1C, MORC1, DPPA4, DPPA2</i>
	ECA23 (4.25)	<i>ALDH1A1, MIR204B-2, MIR8951, C23H9orf57, APBA1, PTAR1, CFAP95, MAMDC2, SMC5, CEMIP2, C23H9orf85, TRPM6, FAM189A2, KLF9, TRPM3, ABHD17B, GDA, ZFAND5, RORB, C23H9orf40, TMC1</i>
NUML	ECA5 (14.06)	<i>NECTIN4, PPOX, CCDC190, NCSTN, PBX1, VANGL2, KLHDC9, FCER1G, ADAMTS4, MIR7177A, ATF6, PCP4L1, SLAMF9, FCRLB, F11R, NIT1, TOMM40L, CFAP126, ARHGAP30, UFC1, USP21, B4GALT3, NDUF52, APOA2, NR1I3, SDHC, RGS5, HSD17B7, CD244, LY9, SLAMF7, UHMK1, CD84, SPATA46, SLAMF6, PEX19, LMX1A, PEA15, NUF2, CASQ1, RGS4, ATP1A4, DDR2, ATP1A2, SH2D1B, IGSF8, KCNJ9, KCNJ10, PIGM, IGSF9, CFAP45, CD48, SLAMF1, COPA, DCAF8, TAGLN2, HSPA6, FCRLA, OLFML2B, DUSP12, MPZ, TSTD1, USF1, PFDN2, DEDD, NHLH1</i>
	ECA11 (8.48)	<i>TP53, AURKB, PER1, ALOXE3, ALOX12B, ALOX15, ALOX15B, SHBG, DVL2, MYH1, MYH2, SLC2A4, EFN3, TNFSF13, MIR195, MIR497, MIR324, MIR9096, TNFSF12, SPEM2, TMEM220, RNASEK, FXR2, BCL6B, KCTD11, WRAP53, FGF11, PHF23, DNAH2, ADPRM, SCO1, GAS7, GLP2R, DHRS7C, USP43, STX8, NTN1, MFSD6L, KRBA2, ODF4, ARHGEF15, CTC1, VAMP2, GUCY2D, CHD3, KDM6B, ATP1B2, SAT2, POLR2A, SLC35G6, CHRNB1, SPEM1, NLGN2, PLSCR3, TMEM95, ACAP1, YBX2, CLDN7, ELP5, CTDNEP1, ASGR2, SLC16A11, SLC16A13, C11H17orf49, PELP1, PIRT, MYH3, MYH8, MYH13, CFAP52, PIK3R5, PIK3R6, CCDC42, MYH10, NDEL1, RNF222, RPL26, RANGRF, SLC25A35, PFAS, BORCS6, TMEM107, CNTROB, CYB5D1, NAA38, TMEM88, TMEM102, TMEM256, TNK1, NEURL4, GPS2, ACADVL, DLG4, ASGR1, GABARAP, GSG1L2, SENP3, EIF5A, RCVRN, SOX15, ZBTB4, MYH4, HES7, TRAPPC1, KCNAB3, MPDU1, EIF4A1, CD68</i>
NUMR	ECA7 (81.96)	<i>RHOG, UCP3, IL18BP, UCP2, SLCO2B1, MIR139, MIR326, COA4, ATG16L2, TRIM21, ART5, ANAPC15, FOLR1, FOLR2, INPPL1, CLPB, FCHSD2, P2RY2, ARHGEF17, RELT, PLEKHB1, RAB6A, MRPL48, C2CD3, PPME1, P4HA3, KCNE3, LIPT2, CHRDL2, RNF169, NEU3, ARRB1, KLHL35, GDPD5, SERPINH1, MAP6, MOGAT2, RRM1, STIM1, PGAP2, NUP98, ART1, NUMA1, LAMTOR1, FOLR3, PHOX2A, PDE2A, ARAP1, STARD10, FAM168A, PAAF1, PGM2L1, POLD3, SPCS2, RPS3, OR52B3, TPBGL, P2RY6, OR52B37P, OR52M2, OR52P2, OR51AE1, OR52B4OP, OR52B4F, OR52B4GP, OR52B4E, OR52B4, OR55B1, CHRNA10, RNF121, XRR1, OR2AT2, OR2AT2D, OR2AT2EP, OR2AT13P, OR52K1, OR52B4N, OR52B4D, DNAJB13</i>

POS: position of hair whorls on the head; NUM: number of hair whorls on the head; NUML and NUMR: number of hair whorls on the left and right side of the neck, respectively.

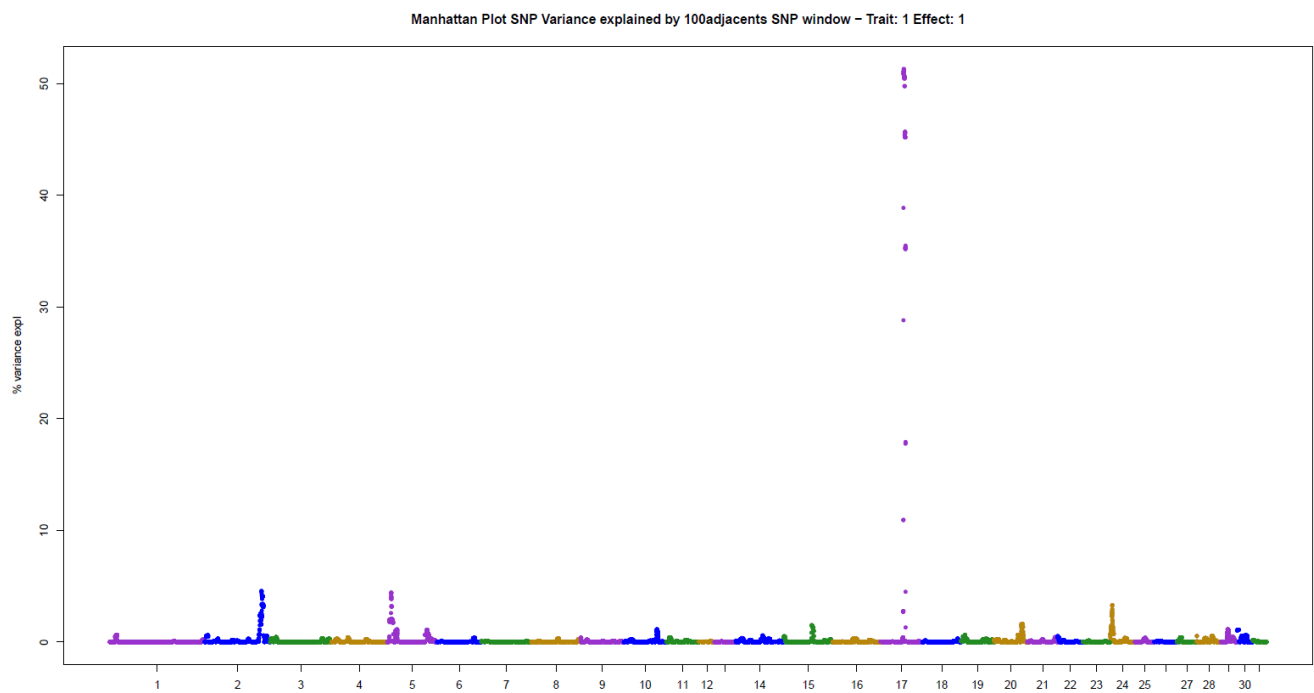


Figure 2. Manhattan plot of hair whorl position on the head of Quarter Horses. The y-axis indicates the proportion of variance explained by windows of 100 adjacent SNPs. The chromosomes are given on the x-axis.

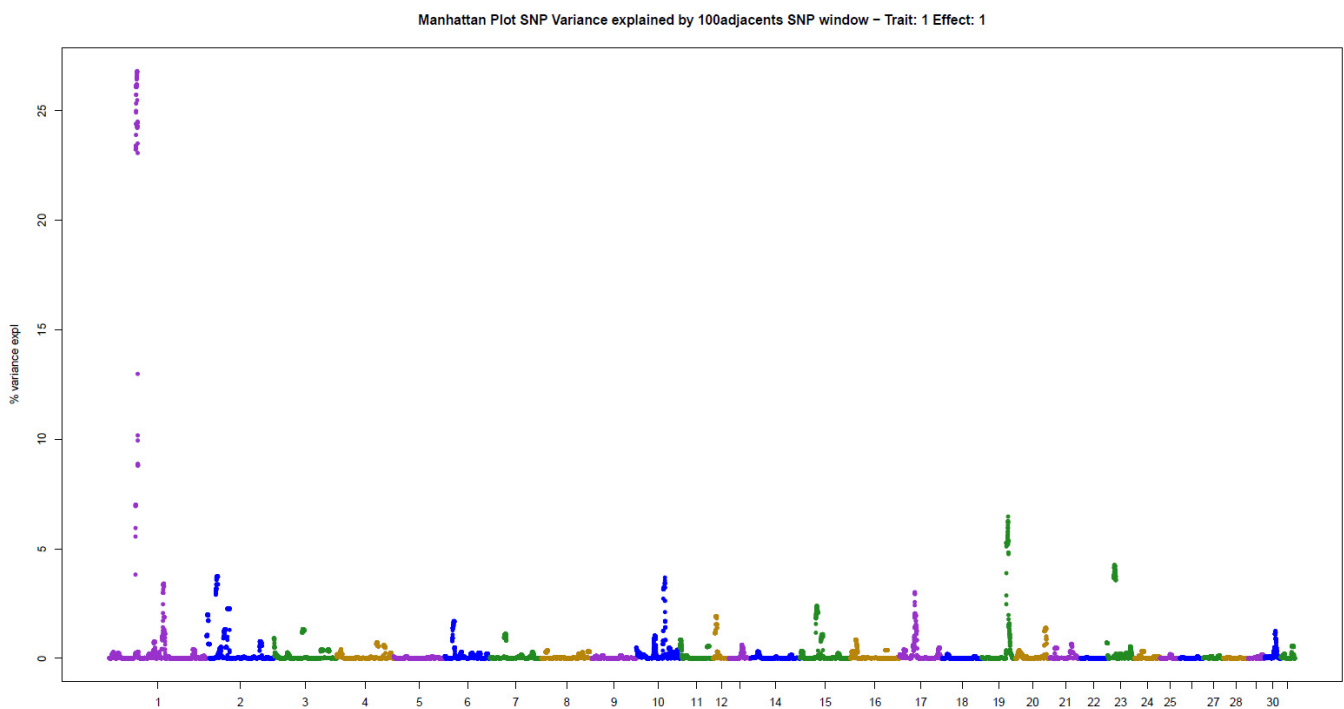


Figure 3. Manhattan plot of hair whorl number on the head of Quarter Horses. The y-axis indicates the proportion of variance explained by windows of 100 adjacent SNPs. The chromosomes are given on the x-axis.

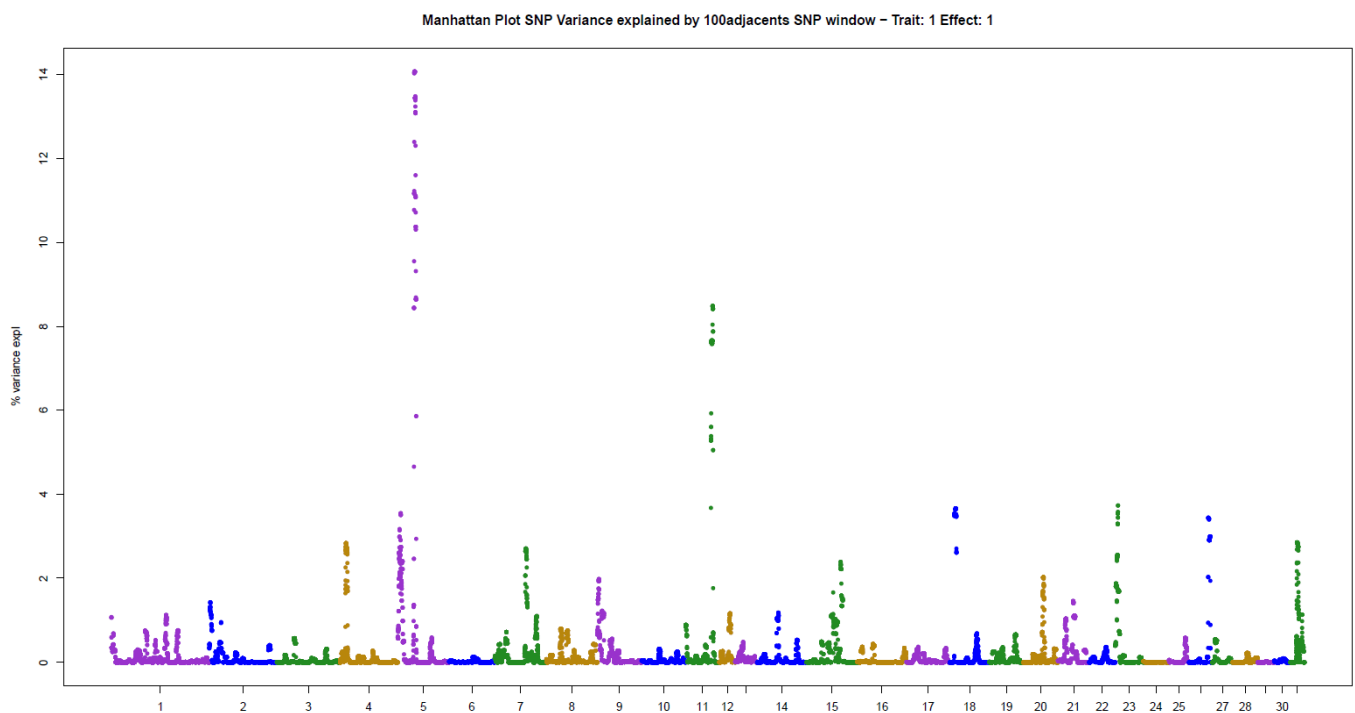


Figure 4. Manhattan plot of hair whorl number on the left side of the neck of Quarter Horses. The y-axis indicates the proportion of variance explained by windows of 100 adjacent SNPs. The chromosomes are given on the x-axis.

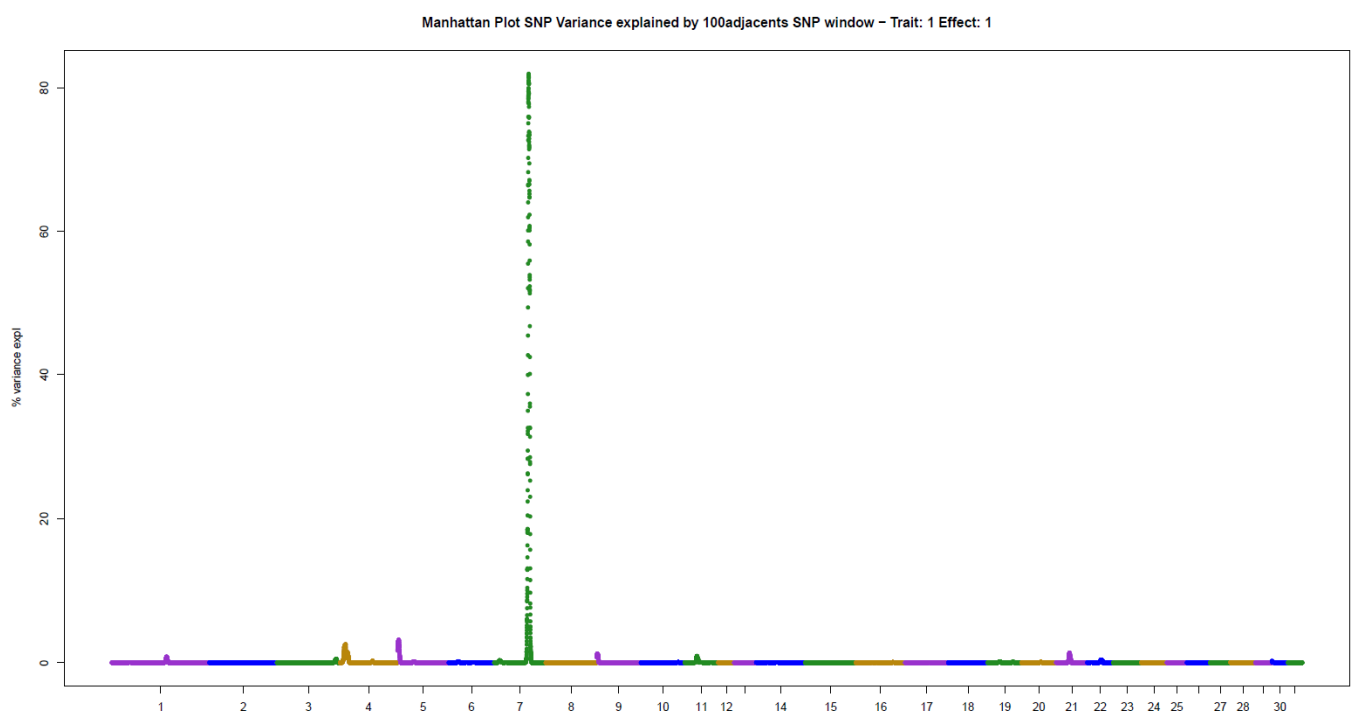


Figure 5. Manhattan plot of hair whorl number on the right side of the neck of Quarter Horses. The y-axis indicates the proportion of variance explained by windows of 100 adjacent SNPs. The chromosomes are given on the x-axis.

4. Discussion

This is the first GWAS of hair whorl traits in domestic animals, using horses as a study model. Hair whorl traits are used as indicators of behavior in horses [3–6]. The genetic architecture of these traits was very similar, with few genomic regions explaining much

of the additive genetic variance in the traits. There were between one and three genomic windows that explained more than 4% of the additive variance for each trait. Together, these windows explained 20% to 80% of the additive variance in the traits analyzed. The main genomic windows associated with the different whorl phenotypes were not the same. However, the traits are highly correlated with one another [10]. This indicates that gene groups influence the traits to different extents. Similar results have been reported in the literature for other genetically correlated traits [13].

For POS, the window that explained most of the additive variance was located on ECA17. This window harbors the *KLF5* gene, which is known for its role in epidermal biology, as well as controlling repair and growth in the root of the hair follicle in humans [14]. This gene may therefore play a role in hair whorl formation. Curiously, this gene has been associated with chronic schizophrenia in humans [15]. This is an interesting fact, since hair whorl position on the head of animals, including horses, has been associated with behavior. This finding can be attributed to the pleiotropic effect of this major-effect gene. Another gene with an action similar to that of *KLF5* was found in the second window for POS, located on ECA2. The *IL2* gene is related to hair follicle growth, and has been associated with hair loss (alopecia) in humans [16]. In addition, an association with multiple sclerosis [17] and schizophrenia [18] has been reported, demonstrating its pleiotropic effect.

Candidate genes found in the main windows associated with hair whorl position on the head of horses exert an effect on the formation and growth of hair follicles, and might be associated with whorl formation. Interestingly, the genes identified here have a pleiotropic effect on psychiatric characteristics. This is the first indication of biological and physiological activity that provides a plausible explanation for hair whorl position as an indicator of behavior. Furthermore, it is the beginning of the observation/validation of the genetic mechanisms underlying the phenotypic observation.

For NUM, the window explaining most of the additive variance, located on ECA1, contains the *SIRT1* gene, which is expressed in the hair follicle [19,20], and may participate in hair whorl formation. This gene has also been associated with depression and schizophrenia [21]. Other genes with an action similar to that of *SIRT1* were found in the second window for NUM. The *CD47* gene is known for its biological role in follicular development and hair follicle formation [22], in addition to activity in the central nervous system, participating in the cortical development of neurons [23] and regulating recovery processes in the central nervous system after severe injuries in humans [24]. The *CD200* gene is expressed in hair follicle stem cells [25], and is related to schizophrenia-like alterations in animals [26], in addition to Parkinson's disease [27]. The third window for NUM, located on ECA23, contains the *ALDH1A1* gene, which is involved in signaling processes and morphogenesis of the hair follicle [28]. An association with Parkinson's disease has also been reported [29].

Similar to the position trait, genes associated with the number of hair whorls on the head exert activity in both the hair follicle and neurodegenerative diseases, which are indicators of behavioral and neurological alterations. The number of hair whorls on the head has also been associated with behavior in horses [7], providing additional evidence of the interrelationship between these phenotypes.

Analysis of the main window associated with NUML, located on ECA5, revealed a series of genes expressed in the hair follicle: *NECTIN4* [30], *PPOX* [31], *CCDC190* [32], *NCSTN* [33], *PBX1* [34], *VANGL2* [35] and *KLHDC9* [32]. The number of hair whorls on the neck has not yet been associated with behavioral traits, but there is evidence of neurological action of some of the cited genes: *NCSTN* [36], *PBX1* [37,38], and *VANGL2* [39]. A series of genes expressed in the hair follicle were also found in the second window, located on ECA11: *TP53* [40], *AURKB* [41], *PER1* [42], *ALOXE3* and *ALOX12B* [43] and *DVL2* [44]. Some of these genes are associated with hair loss: *ALOX15B* [45], *SHBG* [46], and *ALOX15* [47]. In addition, there is evidence of neurological action of some of the genes identified in the second window: *PER1* [48], *SHBG* [49,50], and *DVL2* [51].

For NUMR, some genes related to hair follicle development and growth were found in the window that explained the highest proportion of variance, located on ECA7; these are listed as candidates: *RHOG* [52], *UCP2* [53], *UCP3* [54] and *IL18BP* [55]. Although this trait has not been associated with behavior, some of the genes found also exhibit neuropsychiatric actions: *RHOG* [56], *UCP2* [57], and *UCP3* [58].

Unfortunately, the low SNP density leads to large genomic windows with many genes. This makes it difficult to identify reliable candidates. The use of high-density panels would improve finding them and fine-map causative mutations.

5. Conclusions

Genomic regions associated with hair whorl traits in horses were identified in the present study. In these regions, many genes whose metabolic activity is related to hair follicle growth were prospected, and they were indicated as candidates that may influence these traits. Curiously, some of these genes also have known neurological and behavioral functions. The possible pleiotropic effect of these genes is the first indication of genetic–biological validation and elucidation of the association between hair whorls and temperament in animals.

Author Contributions: D.F.P.d.A.L.: Software, Formal Analysis, Investigation, Writing—Original Draft, Writing—Review and Editing. V.A.R.d.C.: Software, Formal Analysis, Investigation, Writing—Review and Editing. G.L.P.: Data Collection, Data Curation, Methodology, Writing—Review and Editing. R.A.C.: Project Administration, Data Collection, Data Curation, Writing—Review and Editing. R.B.C.: Software, Investigation, Methodology, Writing—Review and Editing. G.M.F.d.C.: Conceptualization, Supervision, Validation, Writing—Review and Editing. All authors have read and agreed to the published version of the manuscript.

Funding: This research was funded by “Fundação de Amparo à Pesquisa do Estado de São Paulo” (Fapesp), Brazil, (Grant 2014/20207-1) and the fellowship granted for the first author was provided “Fundação de Amparo à Pesquisa do Estado da Bahia” (Fapesb), Brazil.

Data Availability Statement: The data presented in this study are available on request from the Rogério Abdallah Curi.

Acknowledgments: The authors thank the Brazilian Association of Quarter Horse Breeders (ABQM, in Portuguese acronym) for kindly proving the data.

Conflicts of Interest: The authors declare that there are no conflict of interest.

References

1. ABQM—Associação Brasileira de Criadores de Cavalos Quarto de Milha. Quarto de Milha: O Cavalos da Família Brasileira. Cartilha ABQM, 2016. Available online: http://www.abqm.com.br/documentos/institucional/abqm_cartilha.pdf (accessed on 27 June 2021).
2. Wickens, C.; Brooks, S.A. Genetics of equine behavioral traits. *Vet. Clin. N. Am. Equine Pract.* **2020**, *36*, 411–424. [[CrossRef](#)]
3. Randle, H.D. Facial hair whorl position and temperament in cattle. *Appl. Anim. Behav. Sci.* **1998**, *56*, 139–147. [[CrossRef](#)]
4. Górecka, A.; Golonka, M.; Chruszczewski, M.; Jezierski, T. A note on behaviour and heart rate in horses differing in facial hair whorl. *Appl. Anim. Behav. Sci.* **2007**, *105*, 244–248. [[CrossRef](#)]
5. Murphy, J.; Arkins, S. Facial hair whorls (trichoglyphs) and the incidence of motor laterality in the horse. *Behav. Process.* **2008**, *79*, 7–12. [[CrossRef](#)]
6. Shivley, C.; Grandin, T.; Deesing, M. Behavioral laterality and facial hair whorls in horses. *J. Equine Vet. Sci.* **2016**, *44*, 62–66. [[CrossRef](#)]
7. Furdon, S.A.; Clark, D.A. Scalp hair characteristics in the newborn infant. *Adv. Neonatal Care* **2003**, *3*, 286–296. [[CrossRef](#)]
8. Górecka, A.; Słoniewski, K.; Golonka, M.; Jaworski, Z.; Jezierski, T. Heritability of hair whorl position on the forehead in Konik horses. *J. Anim. Breed. Genet.* **2006**, *123*, 396–398. [[CrossRef](#)] [[PubMed](#)]
9. Yokomori, T.; Tozaki, T.; Mita, H.; Miyake, T.; Kakoi, H.; Kobayashi, Y.; Kusano, K.; Itou, T. Heritability estimates of the position and number of facial hair whorls in thoroughbred horses. *BMC Res. Notes* **2019**, *12*, 1–4. [[CrossRef](#)]
10. Cruz, V.A.R.; Lima, D.F.P.A.; Diaz, I.P.S.; Curi, R.A.; Pereira, G.L.; Costa, R.B.; de Camargo, G.M.F. Genetic parameters for hair whorl traits in horses. *Livest. Sci.* **2021**, *252*, 104679. [[CrossRef](#)]

11. Pereira, G.L.; Chud, T.C.; Bernardes, P.A.; Venturini, G.C.; Chardulo, L.A.; Curi, R.A. Genotype imputation and accuracy evaluation in racing quarter horses genotyped using different commercial SNP panels. *J. Equine Vet. Sci.* **2017**, *58*, 89–96. [[CrossRef](#)]
12. Tsuruta, S.; Misztal, I. THRGIBBS1F90 for estimation of variance components with threshold-linear models. Commun. 27–31. In Proceedings of the 8th World Congress on Genetics Applied to Livestock Production, Belo Horizonte, Brazil, 13–18 August 2006.
13. Irano, N.; de Camargo, G.M.F.; Costa, R.B.; Terakado, A.P.N.; Magalhaes, A.; Silva, R.M.D.O.; Dias, M.M.; Bignardi, A.B.; Baldi, F.; Carvalheiro, R.; et al. Genome-wide association study for indicator traits of sexual precocity in Nellore cattle. *PLoS ONE* **2016**, *11*, e0159502. [[CrossRef](#)]
14. Sur, I.; Undén, A.B.; Toftgård, R. Human Krüppel-like factor5/KLF5: Synergy with NF- κ B/Rel factors and expression in human skin and hair follicles. *Eur. J. Cell Biol.* **2002**, *81*, 323–334. [[CrossRef](#)]
15. Yanagi, M.; Hashimoto, T.; Kitamura, N.; Fukutake, M.; Komure, O.; Nishiguchi, N.; Kawamata, T.; Maeda, K.; Shirakawa, O. Expression of Kruppel-like factor 5 gene in human brain and association of the gene with the susceptibility to schizophrenia. *Schizophr. Res.* **2008**, *100*, 291–301. [[CrossRef](#)] [[PubMed](#)]
16. Jabbari, A.; Petukhova, L.; Cabral, R.M.; Clynes, R.; Christiano, A.M. Genetic basis of alopecia areata. A roadmap for translational research. *Dermatol. Clin.* **2013**, *31*, 109–117. [[CrossRef](#)] [[PubMed](#)]
17. Al-Naseri, M.A.S.; Ad’hiah, A.H.; Salman, E.D. The association between multiple sclerosis and genetic variations of *TGF β 1* and *IL2* genes in Iraqi patients. *Meta Gene* **2019**, *19*, 253–257. [[CrossRef](#)]
18. Tan, B.; Yatim, S.M.J.; Peng, S.; Gunaratne, J.; Hunziker, W.; Ludwig, A. The mammalian crumbs complex defines a distinct polarity domain apical of epithelial tight junctions. *Curr. Biol.* **2020**, *30*, 2791–2804. [[CrossRef](#)] [[PubMed](#)]
19. Liu, J.; Xu, Y.; Wu, Q.; Ding, Q.; Fan, W. Sirtuin-1 protects hair follicle stem cells from TNF α -mediated inflammatory stress via activating the *MAPK-ERK-Mfn2* pathway. *Life Sci.* **2018**, *212*, 213–224. [[CrossRef](#)] [[PubMed](#)]
20. Kim, J.; Kim, M.-M. The effect of emodin on melanogenesis through the modulation of ERK and MITF signaling pathway. *Nat. Prod. Res.* **2020**, 1–5. [[CrossRef](#)]
21. Wang, D.; Tang, W.; Zhao, J.; Fan, W.; Zhang, Y.; Zhang, C. A comprehensive analysis of the effect of SIRT1 variation on the risk of schizophrenia and depressive symptoms. *Front. Genet.* **2020**, *11*, 832. [[CrossRef](#)]
22. Gnedeva, K.; Vorotelyak, E.; Cimadamore, F.; Cattarossi, G.; Giusto, E.; Terskikh, V.V.; Terskikh, A.V. Derivation of hair-inducing cell from human pluripotent stem cells. *PLoS ONE* **2015**, *10*, e0116892. [[CrossRef](#)]
23. Numakawa, T.; Ishimoto, T.; Suzuki, S.; Numakawa, Y.; Adachi, N.; Matsumoto, T.; Yokomaku, D.; Koshimizu, H.; Fujimori, K.; Hashimoto, R.; et al. Neuronal roles of the integrin-associated protein (*IAP/CD47*) in developing cortical neurons. *J. Biol. Chem.* **2004**, *279*, 43245–43253. [[CrossRef](#)]
24. Zhao, S.; Yu, Z.; Liu, Y.; Bai, Y.; Jiang, Y.; van Leyen, K.; Yang, Y.-G.; Lok, J.M.; Whalen, M.J.; Lo, E.H.; et al. *CD47* deficiency improves neurological outcomes of traumatic brain injury in mice. *Neurosci. Lett.* **2017**, *643*, 125–130. [[CrossRef](#)] [[PubMed](#)]
25. Zaki AK, A.; Almundarij, T.I.; Abo-Aziza, F.A. Comparative characterization and osteogenic/adipogenic differentiation of mesenchymal stem cells derived from male rat hair follicles and bone marrow. *Cell Regen.* **2020**, *9*, 1–14.
26. Chamera, K.; Szuster-Głuszczyk, M.; Trojan, E.; Basta-Kaim, A. Maternal immune activation sensitizes male offspring rats to lipopolysaccharide-induced microglial deficits involving the dysfunction of *CD200-CD200R* and *CX3CL1-CX3CR1* systems. *Cells* **2020**, *9*, 1676. [[CrossRef](#)] [[PubMed](#)]
27. Rao, J.S.; Kim, H.W.; Kellom, M.; Greenstein, D.; Chen, M.; Kraft, A.D.; Harry, G.J.; Rapoport, S.J.; Basselin, M. Increased neuroinflammatory and arachidonic acid cascade markers, and reduced synaptic proteins, in brain of HIV-1 transgenic rats. *J. Neuroinflamm.* **2011**, *8*, 1–13. [[CrossRef](#)] [[PubMed](#)]
28. Everts, H.B.; Sundberg, J.P.; King, L.E.; Ong, D.E. Immunolocalization of enzymes, binding proteins, and receptors sufficient for retinoic acid synthesis and signaling during the hair cycle. *J. Investig. Dermatol.* **2007**, *127*, 1593–1604. [[CrossRef](#)]
29. Grünblatt, E.; Ruder, J.; Monoranu, C.M.; Riederer, P.; Youdim, M.B.; Mandel, S.A. Differential alterations in metabolism and proteolysis-related proteins in human Parkinson’s disease substantia nigra. *Neurotox. Res.* **2017**, *33*, 560–568. [[CrossRef](#)]
30. Murata, M.; Ito, T.; Tanaka, Y.; Kaku-Ito, Y.; Furue, M. *Nectin4* expression in extramammary paget’s disease: Implication of a new therapeutic target. *Int. J. Mol. Sci.* **2020**, *21*, 5891. [[CrossRef](#)]
31. Shah, K.; Mehmood, S.; Jan, A.; Abbe, I.; Ali, R.H.; Khan, A.; Chishti, M.S.; Lee, K.; Ahmad, F.; Ansar, M.; et al. Sequence variants in nine different genes underlying rare skin disorders in 10 consanguineous families. *HHS Public Access* **2018**, *56*, 1406–1413. [[CrossRef](#)]
32. Cho, W.K.; Kim, H.; Paek, S.H.; Kim, S.; Seo, H.H.; Song, J.; Lee, O.H.; Min, J.; Lee, S.J.; Jo, Y.; et al. Gene expression profile of human follicle dermal papilla cells in response to *Camellia japonica* phytoplacenta extract. *FEBS Open Bio* **2021**, *11*, 633–651. [[CrossRef](#)]
33. Nishimori, N.; Hayama, K.; Kimura, K.; Fujita, H.; Fujiwara, K.; Terui, T. A novel *ncstn* gene mutation in a japanese family with hidradenitis suppurativa. *Acta Derm. Venereol.* **2020**, *100*, 2–3. [[CrossRef](#)]
34. Wang, B.; Liu, F.; Liu, Z.; Han, X.; Lian, A.; Zhang, Y.; Zuo, K.; Wang, Y.; Liu, M.; Zou, F.; et al. Internalization of the TAT-PBX1 fusion protein significantly enhances the proliferation of human hair follicle-derived mesenchymal stem cells and delays their senescence. *Biotechnol. Lett.* **2020**, *42*, 1877–1885. [[CrossRef](#)]
35. Cetera, M.; Leybova, L.; Woo, F.W.; Deans, M.; Devenport, D. Planar cell polarity-dependent and independent functions in the emergence of tissue-scale hair follicle patterns. *Dev. Biol.* **2017**, *428*, 188–203. [[CrossRef](#)] [[PubMed](#)]

36. Herrera-Rivero, M.; Hernández-Aguilar, M.E.; Aranda-Abreu, G.E. A strategy focused on MAPT, APP, NCSTN and BACE1 to build blood classifiers for Alzheimer's disease. *J. Theor. Biol.* **2015**, *376*, 32–38. [[CrossRef](#)] [[PubMed](#)]
37. Grebbin, B.M.; Hau, A.C.; Groß, A.; Anders-Maurer, M.; Schramm, J.; Koss, M.; Wille, C.; Mittelbronn, M.; Selleri, L.; Schulte, D. PBX1 is required for adult subventricular zone neurogenesis. *Development* **2016**, *143*, 2281–2291. [[PubMed](#)]
38. Wang, M.; Zhang, Y.; Feng, L.; Zheng, J.; Fan, S.; Liu, J.; Yang, N.; Liu, Y.; Zuo, P. Compound porcine cerebroside and ganglioside injection attenuates cerebral ischemia–reperfusion injury in rats by targeting multiple cellular processes. *Neuropsychiatr. Dis. Treat.* **2017**, *13*, 927–935. [[CrossRef](#)]
39. Carvalho, S.D.S.; Moreau, M.M.; Hien, Y.E.; Garcia, M.; Aubailly, N.; Henderson, D.J.; Studer, V.; Sans, N.; Thoumine, O.; Montcouquiol, M. *Vangl2* acts at the interface between actin and N-cadherin to modulate mammalian neuronal outgrowth. *Elife* **2020**, *9*, e51822. [[CrossRef](#)] [[PubMed](#)]
40. Xu, Z.; He, X.; Shi, X.; Xia, Y.; Liu, X.; Wu, H.; Li, P.; Zhang, H.; Yin, W.; Du, X.; et al. Analysis of differentially expressed genes among human hair follicle-derived iPSCs, induced hepatocyte-like cells, and primary hepatocytes. *Stem Cell Res. Ther.* **2018**, *9*, 211. [[CrossRef](#)] [[PubMed](#)]
41. Hardman, J.A.; Haslam, I.; Farjo, N.; Farjo, B.; Paus, R. Thyroxine differentially modulates the peripheral clock: Lessons from the human hair follicle. *PLoS ONE* **2015**, *10*, e0121878. [[CrossRef](#)]
42. Sugiura, K.; Akiyama, M. Update on autosomal recessive congenital ichthyosis: MRNA analysis using hair samples is a powerful tool for genetic diagnosis. *J. Dermatol. Sci.* **2015**, *79*, 4–9. [[CrossRef](#)]
43. Millar, S.E.; Willert, K.; Salinas, P.C.; Roelink, H.; Nusse, R.; Sussman, D.J.; Barsh, G.S. WNT signaling in the control of hair growth and structure. *Dev. Biol.* **1999**, *207*, 133–149. [[CrossRef](#)]
44. Clements, S.; Techanukul, T.; Lai-Cheong, J.; Mee, J.; South, A.; Pourreya, C.; Burrows, N.; Mellerio, J.; McGrath, J. Mutations in AEC syndrome skin reveal a role for p63 in basement membrane adhesion, skin barrier integrity and hair follicle biology. *Br. J. Dermatol.* **2012**, *167*, 134–144. [[CrossRef](#)]
45. Kozicka, K.; Łukasik, A.; Pastuszczyk, M.; Jaworek, A.; Spałkowska, M.; Kłosowicz, A.; Dyduch, G.; Wojas-Pelc, A. Is hormone testing worthwhile in patients with female pattern hair loss? *Polski Merkuriusz Lekarski* **2020**, *48*, 323–326.
46. Kim, S.-N.; Akindehin, S.; Kwon, H.-J.; Son, Y.-H.; Saha, A.; Jung, Y.-S.; Seong, J.-K.; Lim, K.-M.; Sung, J.-H.; Maddipati, K.R.; et al. Anti-inflammatory role of 15-lipoxygenase contributes to the maintenance of skin integrity in mice. *Sci. Rep.* **2018**, *8*, 1–11. [[CrossRef](#)] [[PubMed](#)]
47. Tong, T.; Kim, N.; Park, T. Topical application of oleuropein induces anagen hair growth in telogen mouse skin. *PLoS ONE* **2015**, *10*, e0129578. [[CrossRef](#)] [[PubMed](#)]
48. López-Olmeda, J.F.; Tartaglione, E.V.; de la Iglesia, H.O.; Sánchez-Vázquez, F.J. Feeding entrainment of food-anticipatory activity and *per1* expression in the brain and liver of zebrafish under different lighting and feeding conditions. *Chronobiol. Int.* **2010**, *27*, 1380–1400. [[CrossRef](#)] [[PubMed](#)]
49. Grasa, M.D.M.; Villarreal, L.; Granero, R.; Vilà, R.; Penelo, E.; Agüera, Z.; Jiménez-Murcia, S.; Romero, M.D.M.; Menchón, J.M.; Remesar, X.; et al. Purging behavior modulates the relationships of hormonal and behavioral parameters in women with eating disorders. *Neuropsychobiology* **2013**, *67*, 230–240. [[CrossRef](#)] [[PubMed](#)]
50. Takayanagi, Y.; Spira, A.P.; McIntyre, R.S.; Eaton, W.W. Sex hormone binding globulin and verbal memory in older men. *Am. J. Geriatr. Psychiatry* **2015**, *23*, 253–260. [[CrossRef](#)] [[PubMed](#)]
51. Inkster, B.; Nichols, T.E.; Saemann, P.G.; Auer, D.P.; Holsboer, F.; Muglia, P.; Matthews, P.M. Pathway-based approaches to imaging genetics association studies: Wnt signaling, GSK3beta substrates and major depression. *Neuroimage* **2010**, *53*, 908–917. [[CrossRef](#)] [[PubMed](#)]
52. Nakrieko, K.A.; Welch, I.; Dupuis, H.; Bryce, D.; Pajak, A.; St Arnaud, R.; Dedhar, S.; D'Souza, S.J.A.; Dagnino, L. Impaired hair follicle morphogenesis and polarized keratinocyte movement upon conditional inactivation of integrin-linked kinase in the epidermis. *Mol. Biol. Cell* **2008**, *19*, 1462–1473. [[CrossRef](#)] [[PubMed](#)]
53. Joost, S.; Annusver, K.; Jacob, T.; Sun, X.; Dalessandri, T.; Sivan, U.; Sequeira, I.; Sandberg, R.; Kasper, M. The molecular anatomy of mouse skin during hair growth and rest. *Cell Stem Cell* **2020**, *26*, 441–457. [[CrossRef](#)] [[PubMed](#)]
54. Mori, S.; Yoshizuka, N.; Takizawa, M.; Takema, Y.; Murase, T.; Tokimitsu, I.; Saito, M. Expression of uncoupling proteins in human skin and skin-derived cells. *J. Investig. Dermatol.* **2008**, *128*, 1894–1900. [[CrossRef](#)]
55. Wang, E.; Chong, K.; Yu, M.; Akhoundsadegh, N.; Granville, D.J.; Shapiro, J.; McElwee, K.J. Development of autoimmune hair loss disease alopecia areata is associated with cardiac dysfunction in C3H/HeJ mice. *PLoS ONE* **2013**, *8*, e62935. [[CrossRef](#)]
56. Lin, X.; Meng, G.; Liu, X.; Yu, T.; Bai, C.; Fei, X.; Deng, S.; Zhao, J.; Ren, S.; Zhang, J.; et al. The differentially expressed genes of human sporadic cerebral cavernous malformations. *World Neurosurg.* **2018**, *113*, e247–e270. [[CrossRef](#)] [[PubMed](#)]
57. Gigante, A.; Andreatza, A.; Lafer, B.; Yatham, L.; Beasley, C.; Young, L. Decreased mRNA expression of uncoupling protein 2, a mitochondrial proton transporter, in post-mortem prefrontal cortex from patients with bipolar disorder and schizophrenia. *Neurosci. Lett.* **2011**, *505*, 47–51. [[CrossRef](#)] [[PubMed](#)]
58. Wang, B.; Zheng, Y.; Shi, H.; Du, X.; Zhang, Y.; Wei, B.; Luo, M.; Wang, H.; Wu, X.; Hua, X.; et al. Zfp462 deficiency causes anxiety-like behaviors with excessive self-grooming in mice. *Genes Brain Behav.* **2016**, *16*, 296–307. [[CrossRef](#)] [[PubMed](#)]